Supporting Information

Structural phase transition in a multi-induced mononuclear Fe^{II} spin-crossover complex

Yuan-Yuan Zhu,*[a] Chang-Wei Liu,[a] Ji Yin,[a] Zhao-Sha Meng,[b] Qian Yang,[b] Junhu Wang,[d] Tao Liu*[c] and Song Gao*[b]

List of Supporting Information

SI1 Synthesis details of the pybox ligand

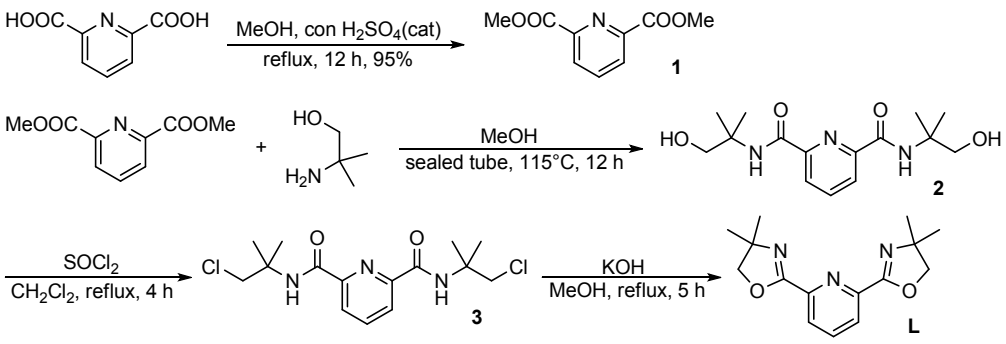

Scheme S1

Compound 1.[1] To pyridine-2,6-dicarboxylic acid (3.34 g, 20 mmol) in methanol (20 mL) was added con. H_2SO_4 (0.5 mL) dropwise and slowly. The solution was stirred at reflux for 12 hours and the insoluble powder was gradually dissolved. After cooled to room temperature, the solution was concentrated under reduced pressure and the crude product was dissolved in EtOAc (30 mL) and washed with deionized H_2O (10 mL × 2), saturated aqueous $NaHCO_3$ (10 mL), and brine (10 mL) and dried over sodium sulfate. The solvent was removed and gave **1** as a white solid (3.70 g, 95%), which was used in the next step without further purification.

Compound 2.[2] A mixture of **1** (1.95 g, 10mmol) and 2-amino-2-methylpropan-1-ol (1.78 g, 20 mmol) and methanol (10 mL) was sealed in a tube and stirred at 115 ºC for 12 h. After cooled to room temperature, the solution was concentrated under reduced pressure. The resulting residue was subjected to column chromatography (SiO_2, dichloromethane/methanol, 20 : 1) to afford **2** as a white solid (2.94 g, 95%). ^{1}H NMR (600 MHz, $CDCl_3$): δ 8.32 (d, J = 7.8 Hz, 2 H), 8.04 (t, J = 7.8 Hz, 1 H), 8.02 (br, 2 H), 3.98 (br, 2 H), 3.72 (d, J = 5.4 Hz, 4 H), 1.47 (s, 12 H).

Compound 3.[3] A solution of **2** (2.94 g, 9.5 mmol) in dichloromethane (10 mL) was cooled in an ice bath, and then $SOCl_2$ (10 mL) was added dropwise. The solution was stirred at reflux for 2 h. After cooled to room temperature, the solution was concentrated under reduced pressure and the resulting residue was triturated with dichloromethane (20 mL). The solution was washed with deionized H_2O (10 mL × 2), saturated aqueous $NaHCO_3$ (10 mL), and brine (10 mL) and dried over anhydrous sodium sulfate. After the solvent was removed, the crude product was subjected to column

chromatography (SiO_2, dichloromethane/EtOAc, 20 : 1) to give **3** as a white solid (2.89 g, 88%). ^{1}H NMR (400 MHz, $CDCl_3$): δ 8.27 (d, J = 7.8 Hz, 2 H), 8.00 (t, J = 7.8 Hz, 1 H), 7.90 (br, 2 H), 3.85 (s, 4 H), 1.55 (s, 12 H).

CompoundL.[3] To a solution of **3** (1.73 g, 5 mmol) in methanol (25 mL) was added KOH (0.7 g, 12.5 mmol). The solution was stirred at reflux for 4 h and white precipitation generated during the reaction. The solution was concentrated under reduced pressure. Then the resulting residue was triturated with dichloromethane (30 mL) and the solution washed with water (15 mL × 3) and brine (15 mL) and dried over anhydrous sodium sulfate. Compound **L** was obtained as a white solid under vacuum drying (1.30 g, 95%). ^{1}H NMR (600 MHz, $CDCl_3$): δ 8.15 (d, J = 7.8 Hz, 2 H), 7.83 (d, J = 7.8 Hz, 1 H), 4.20 (s, 4 H), 1.38 (s, 12 H).

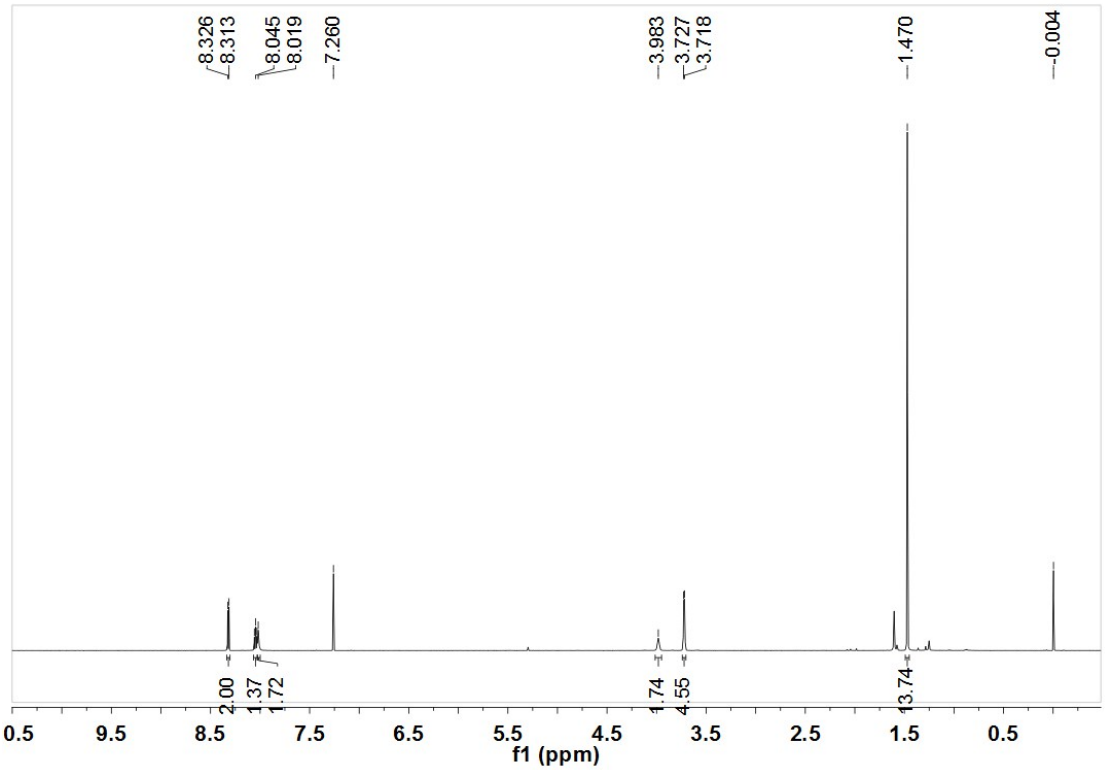

Figure S1. ^{1}H NMR spectrum of compound **2** (600 MHz) in $CDCl_3$ (10 mM).

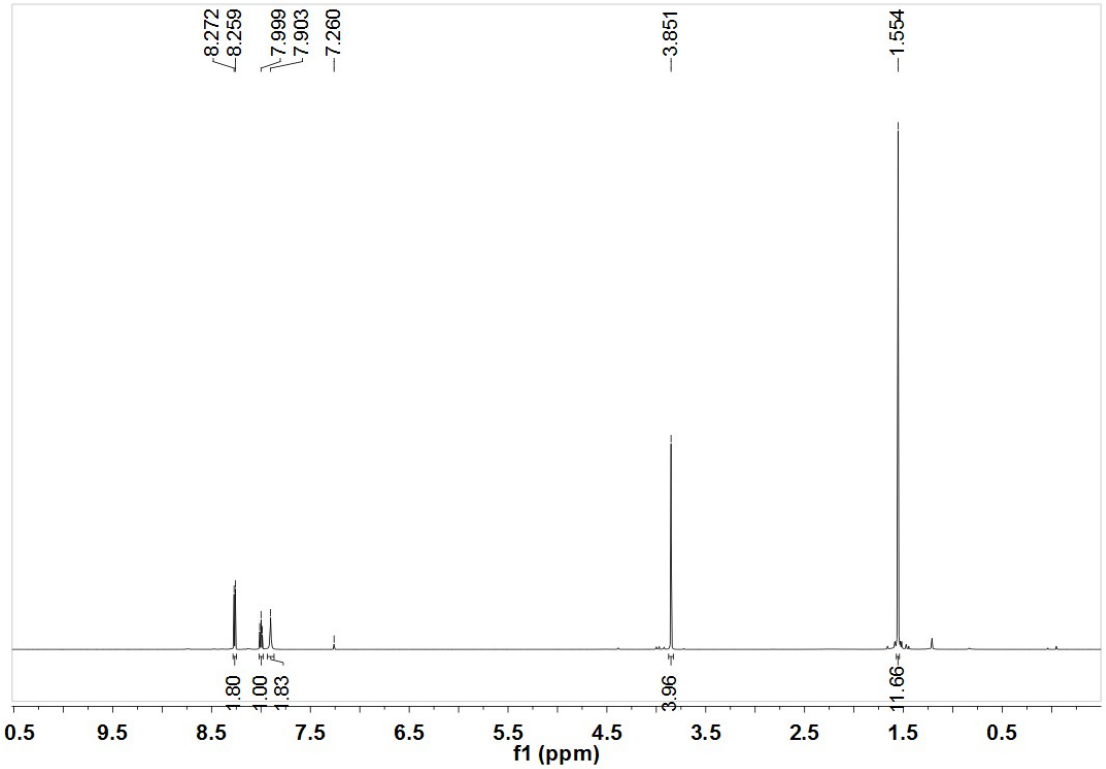

Figure S2. ^{1}H NMR spectrum of compound **3** (600 MHz) in $CDCl_3$ (10 mM).

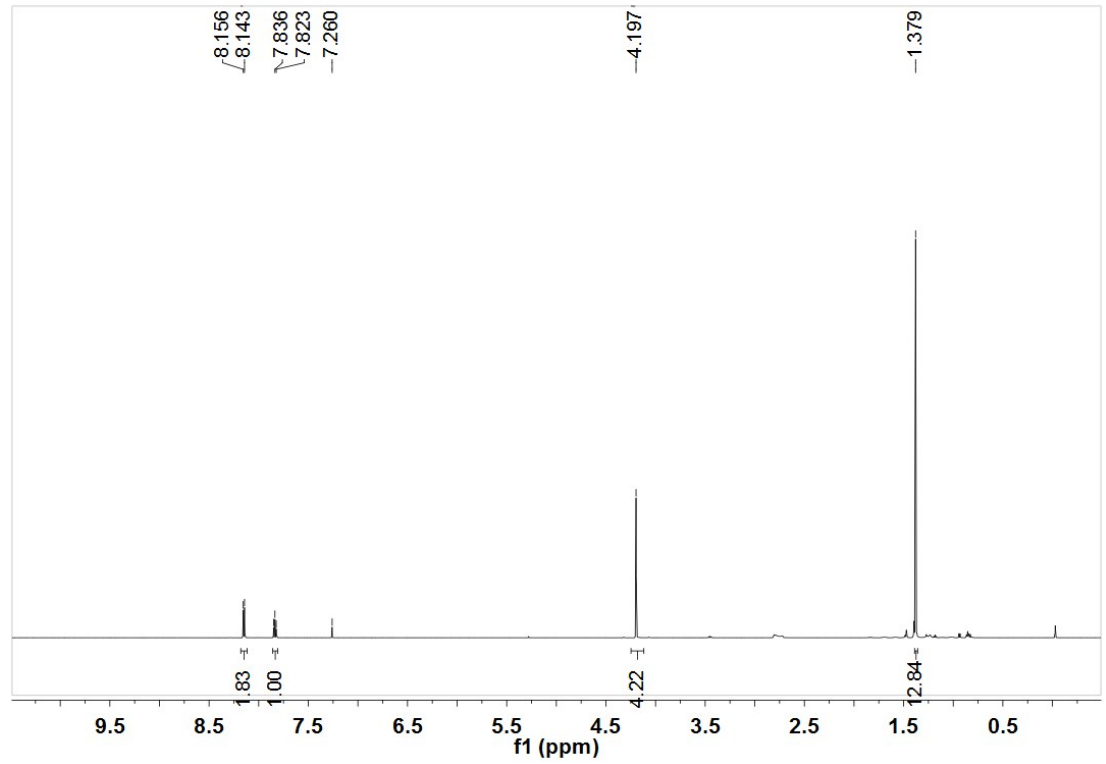

Figure S3. ^{1}H NMR spectrum of compound **L** (600 MHz) in $CDCl_3$ (10 mM).

References

1. Y.-Y. Zhu, C. Cui, N. Li, B.-W. Wang, Z.-M. Wang and S. Gao, *Eur. J. Inorg. Chem*., 2013, **17**, 3101.
2. B. P. Bandgar and S. S. Pandit, *Tetrahedron Lett*., 2003, **44**, 2331.
3. F. Ito, T. Nakamura, S. Yorita, H. Danjo and K. Yamaguchi, *Tetrahedron Lett*., 2009, **50**, 6252.

SI2 Structure details

Table S1. Crystal data, data collection, solution and refinement information of compounds **1a** at different temperatures (250 K, 180 K, 173 K and 100 K) and **1b** (100 K).

	1a (250 K)	**1a** (180 K)	**1a** (173 K)	**1a** (100 K)	**1b** (100 K)
Formula	$C_{30}H_{38}Cl_2FeN_6O_{12}$	$C_{30}H_{38}Cl_2FeN_6O_{12}$	$C_{60}H_{76}Cl_4Fe_2N_{12}O_{24}$	$C_{60}H_{76}Cl_4Fe_2N_{12}O_{24}$	$C_{32}H_{41}Cl_2FeN_7O_{12}$
formula weight	801.41	801.41	1602.82	1602.82	842.47
crystal system	orthorhombic	orthorhombic	monoclinic	monoclinic	orthorhombic
space group	*P*bca	*P*bca	$P2_1/c$	$P2_1/c$	*P*bca
a, Å	13.9412(3)	13.8634(4)	13.909(3)	13.8080(7)	16.9258(4)
b, Å	20.1005(6)	20.0412(5)	20.024(4)	19.7339(9)	19.0959(5)
c, Å	25.5295(8)	25.3447(8)	25.221(5)	25.0603(12)	22.9024(5)
α, deg	90	90	90	90	90
β, deg	90	90	91.79(3)	92.395(5)	90
γ, deg	90	90	90	90	90
V, Å^3	7154.0(3)	7041.8(3)	7021(2)	6822.6(6)	7402.4(3)
Z	8	8	4	4	8
T, K	250.0(1)	180.0(1)	173(2)	100.0(1)	100.0(2)
F(000)	3328	3328	3328	3328	3504
D_C, g cm^{-3}	1.488	1.512	1.516	1.560	1.512
μ, mm^{-1}	0.640	0.650	0.652	0.671	0.623
λ, Å	0.71073	0.71073	0.71073	0.71073	0.71073
crystal size, mm^3	0.32 × 0.21 × 0.20	0.32 × 0.21 × 0.20	0.50 × 0.46 × 0.18	0.32 × 0.21 × 0.20	0.34 × 0.23 × 0.22
T_{min} and T_{max}	0.80923, 1.00000	0.57616, 1.00000	0.8256, 1.0000	0.56507, 1.00000	0.90491, 1.00000
θ_{min}, θ_{max}, deg	3.6230, 28.0520	3.4600, 28.1930	2.3757, 27.4816	3.0410, 27.9130	3.1480, 29.9710
no. total reflns.	31126	37030	15994	29396	29396
no. uniq. reflns, R_{int}	7000, 0.0358	6814, 0.0420	12609, 0.0731	12683, 0.0675	7279, 0.0375
no. obs. [$I \geq 2\sigma(I)$]	5329	5628	7753	10662	5730
no. params	468	468	937	937	496
*R*1 [$I \geq 2\sigma(I)$]	0.0590	0.0658	0.1582	0.1769	0.0397
*wR*2 (all data)	0.1764	0.1806	0.4351	0.4202	0.1013
S	1.069	1.081	1.359	1.169	1.042
$\Delta\rho^a$, e/ Å^3	1.040, –0.837	1.256, –1.029	1.759, –2.076	2.335, – 1.994	0.659, –0.533
max. and mean Δ/σ^b	0.000, 0.000	0.001, 0.000	0.001, 0.000	0.001, 0.000	0.001, 0.000
CCDC	1032872	1032876	1410363	1032884	1032885

[a] Max and min residual density. [b] Max and mean shift/σ.

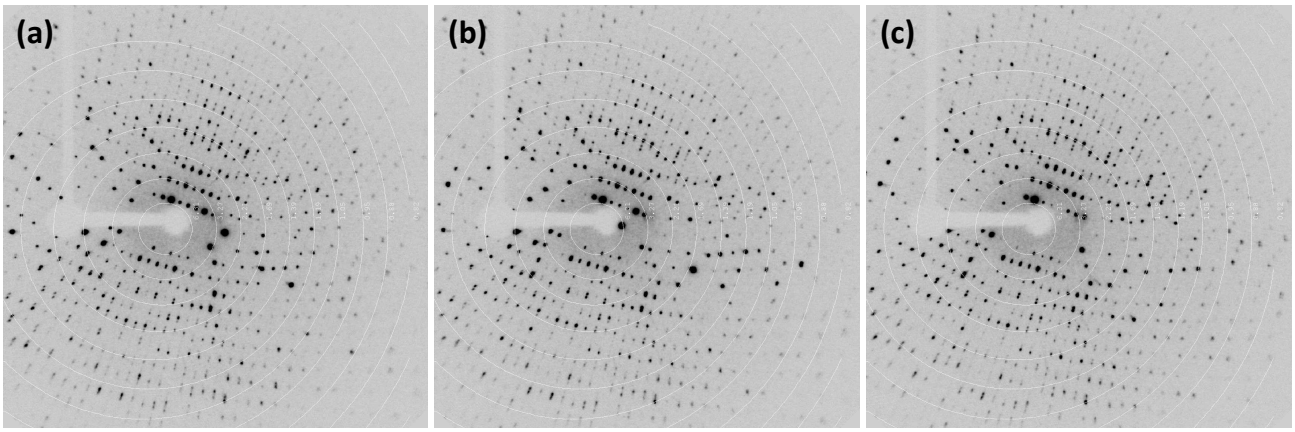

Figure S4. Representative diffraction patterns of **1a** at 100 K, indicating significant twinned crystal phenomenon due to the partial loss of crystallinity after structural phase transition.

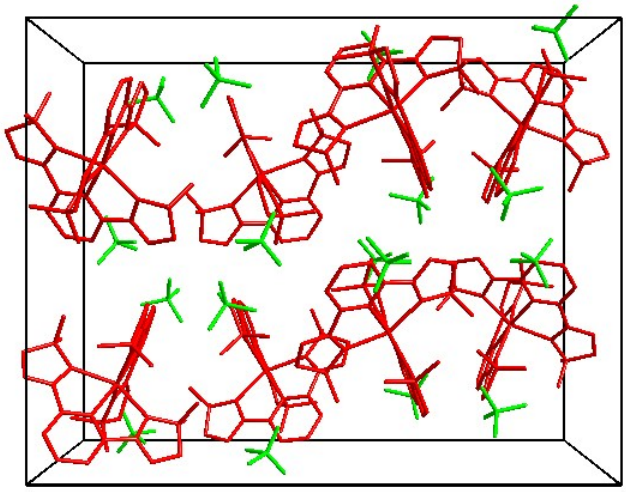

Figure S5. The packing picture of **1a** (250 K) in unit cell along the *a* axis (red: HS Fe^{II} species).

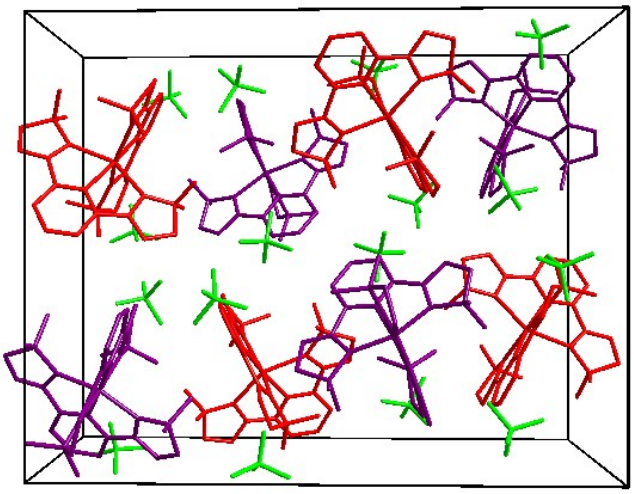

Figure S6. The packing picture of **1a** (100 K) in unit cell along the *a* axis (red: HS Fe^{II} species, purple: LS Fe^{II} species).

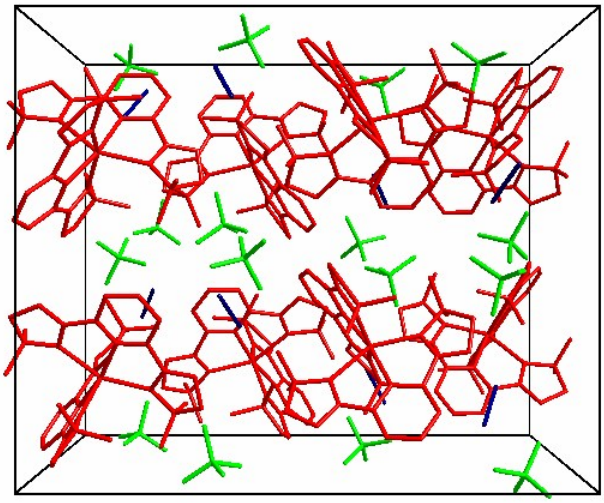

Figure S7. The packing picture of **1b** (100 K) in unit cell along the *a* axis (red: HS Fe^{II} species, green: perchlorate anion, blue: acetonitrile).

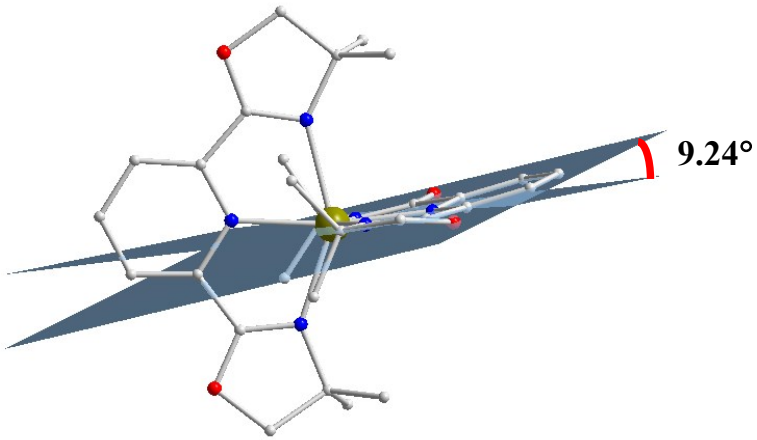

Figure S8. The bending angle between the pyridine ring plane and the pybox ligand plane (determined by three coordinated N atoms in one ligand) in **1b**.

SI3 Properties measurements

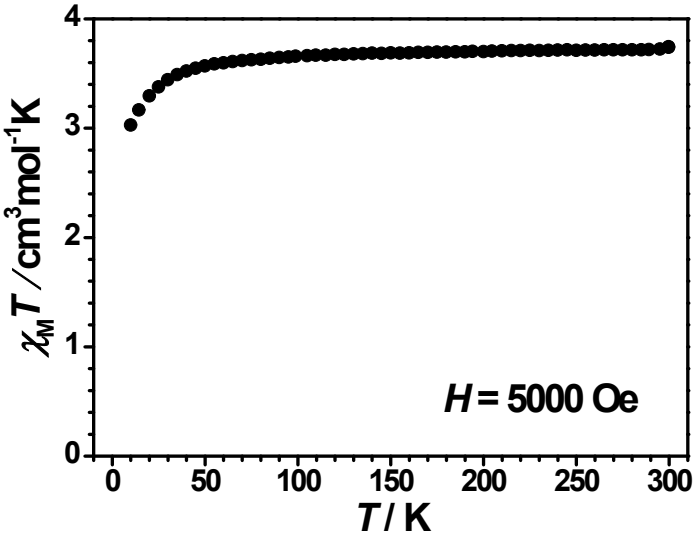

Figure S9. Plots of $\chi_M T$ *vs.* *T* for **1b** in the cooling mode.

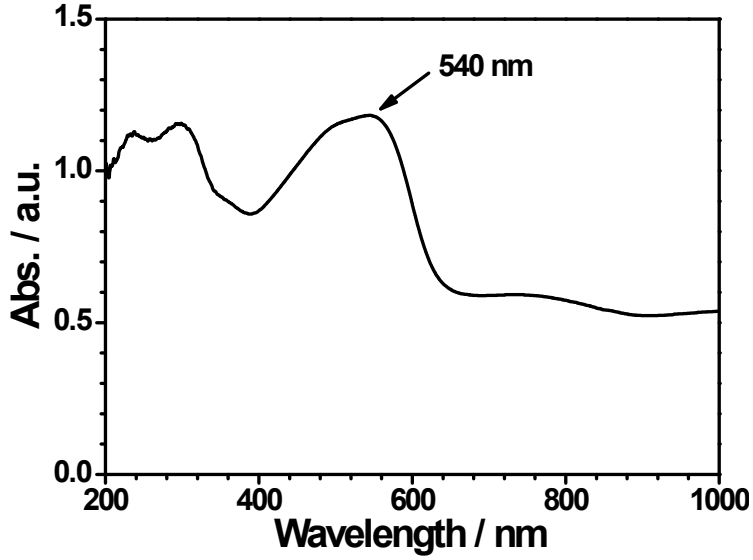

Figure S10. The solid UV-vis spectrum of compound **1a**.

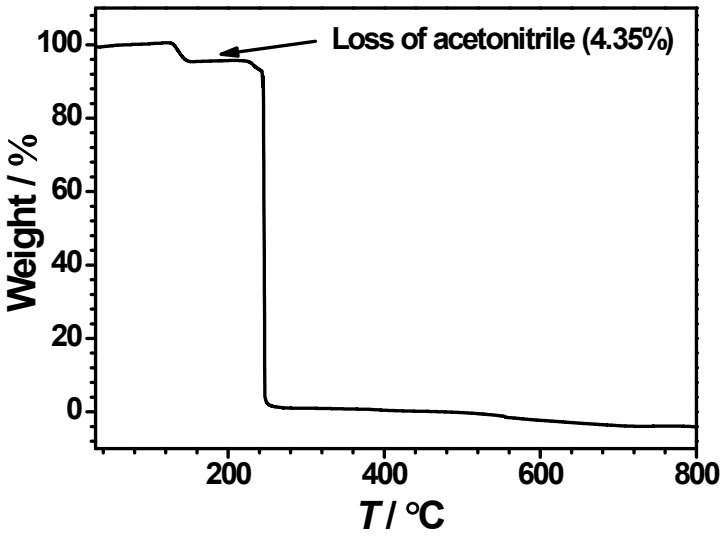

Figure S11. The TGA trace of **1b**, indicating the content of acetonitrile is 4.35% wt, which is consistent with the theoretical value of 4.87% wt.

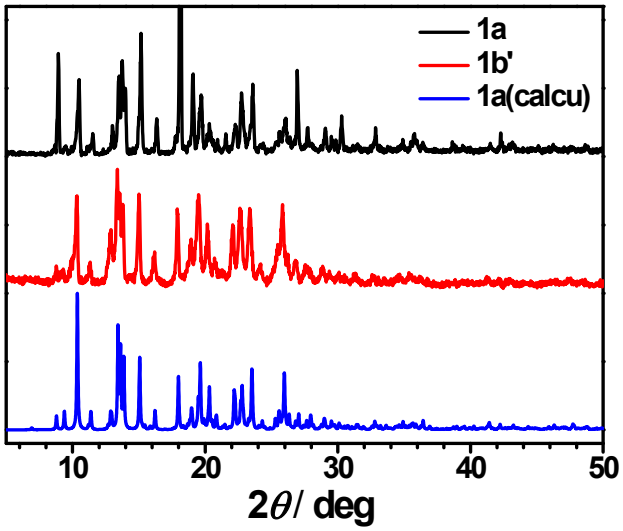

Figure S12. The powder XRD pattern of **1a** and **1b'**, and the simulated pattern from the single-crystal X-ray structure of **1a**.

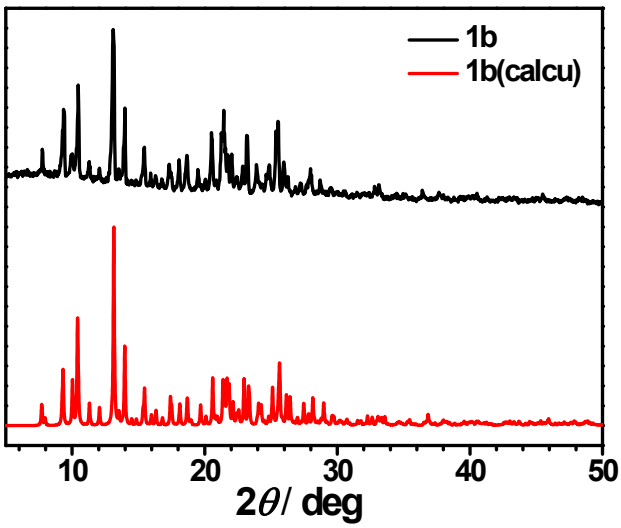

Figure S13. The powder XRD pattern of **1b** and the simulated pattern from the single-crystal X-ray structure.

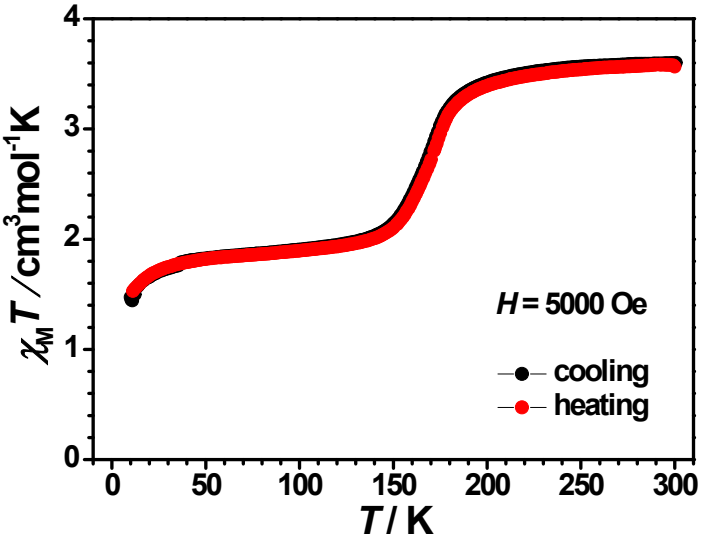

Figure S14. Plots of $\chi_M T$ *vs*. *T* for **1b' (**desolvated sample of **1b)** in the cooling and warming mode.